

Orientation-dependent interactions of DNA with an α -hemolysin channel

Meni Wanunu,¹ Buddhapriya Chakrabarti,² Jérôme Mathé,³ David R. Nelson,² and Amit Meller^{1,*}

¹*Department of Biomedical Engineering and Physics, Boston University, Boston, Massachusetts 02215, USA*

²*Lyman Laboratory of Physics, Harvard University, Cambridge, Massachusetts 02138, USA*

³*Laboratoire de Matériaux Polymères aux Interfaces, Université d'Evry, 91025 Evry, France*

(Received 12 July 2007; revised manuscript received 2 January 2008; published 6 March 2008)

We present experimental and theoretical results on the voltage-dependent escape dynamics of DNA hairpins of different orientations threaded into an α -hemolysin channel. Using a coarse-grained formulation, we map the motion of the polymer in the pore to that of a biased single-particle random walk along the translocation coordinate. By fitting the escape probability distributions obtained from theory to experimental data, we extract the voltage-dependent diffusion constants and bias-induced velocities. Using our two-parameter theory, we obtain excellent agreement with experimentally measured escape time distributions. Further, we find that the ratio of mean escape times for hairpins of different orientations is strongly voltage dependent, with the ratio of 3'- to 5'-threaded DNA decreasing from ≈ 1.7 to ≈ 1 with increasing assisting voltages V_a . We also find that our model describes 5'-threaded DNA escape extremely well, while providing inadequate fits for 3' escape. Finally, we find that the escape times for both orientations are equal for high assisting voltages, suggesting that the interactions of DNA with the α -hemolysin channel are both orientation and voltage dependent.

DOI: [10.1103/PhysRevE.77.031904](https://doi.org/10.1103/PhysRevE.77.031904)

PACS number(s): 87.14.G-, 87.15.Tt

The exploration of biomolecular interactions at the microscopic level has begun to unravel the complex nature of macromolecular interactions. In recent years, nanopores have demonstrated utility in the analysis of biopolymer structure at the single-molecule level. More specifically, the membrane-embedded α -hemolysin (α -HL) toxin channel has been extensively used for probing the translocation dynamics of single-stranded DNA (ssDNA) molecules and other biopolymers, owing to its remarkable robustness and convenient channel size, which allows the threaded entry of single-stranded polynucleotides [1–3]. In these experiments, polynucleotide molecules are voltage driven through the channel, while the electrolyte ion current is recorded. Translocation of individual DNA molecules through the channel is signaled by transient current blockades, corresponding to entry and exit from the pore. Growing experimental evidence suggests that the biopolymer translocation dynamics is governed by the channel-polymer interactions [4,5]. Yet, despite the known structure of α -HL [6], the microscopic nature of these interactions requires further investigation. Aside from fundamental interest in macromolecular interactions, gaining a full understanding of such processes may be valuable for future nanopore devices. In addition to sensing of various analytes, chemically manipulated nanopores [7] may soon be employed to discriminate among individual bases of a translocating polymer, thus fulfilling the quest for rapid, high-throughput DNA sequencing [8,9].

Dynamic voltage control during DNA translocation through nanopores has enabled new types of measurements in which the dynamics is measured, at voltages both below and above the threshold required for initial DNA entry into the channel (~ 50 mV) [10,11]. In particular, this method has enabled measurements of ssDNA escape dynamics from the pore at zero voltage (no bias), revealing a favored

3'-oriented threading over 5' [12]. A coarse-grained model was used to obtain a closed-form expression for $P_s(t)$, the probability that the strand remains in the pore at time t . Using this theory, the diffusion constant $D_{5'}$ was found to be 1.66 times greater than $D_{3'}$, yielding a mean escape time ratio of ≈ 0.6 . However, this orientation dependence at zero bias was found to be strongly suppressed at voltages above 40 mV, with a mere difference of $< 16\%$ in the mean escape time [12]. To date, measurements have been restricted to relatively large voltages, for only two of four possible configurations of ssDNA (with respect to the α -HL pore) [13]. In this voltage regime, the escape dynamics is dominated by voltage-induced drift, rather than diffusion alone. However, it is unclear how diffusion in this regime is affected by the applied voltage.

In this paper, we explore DNA escape at the transition between the bias-free regime ($V=0$ mV) and the high-voltage ($V>40$ mV) limit. Our experiments begin by trapping a ssDNA molecule inside the α -HL channel. We then apply a negative voltage ($V<0$) in order to retract the threaded ssDNA from the pore—defined as an “assisting” field (V_a). We find that poly(dA) molecules inserted with either the 3' or the 5' end into the *cis* side of a α -HL channel behave differently, and, moreover, these differences are voltage dependent. We theoretically account for both 3' and 5' dynamics using a simple, coarse-grained model, which provides a closed-form expression for $P_s(t)$ containing two orientation-dependent free parameters, the long-time diffusion coefficient D and the drift velocity v . Further, we obtain a closed-form expression of the mean escape time by generalizing the formulation of Berg and Purcell [14] to account for voltage-induced drift, and compare it with experimental values.

The trapping of ssDNA in the pore is accomplished using a DNA hairpin, which consists of a poly-(dA)₅₀ overhang tail and a ten base-pair self-complementary duplex region, connected by a six-nucleotide loop. The two

*ameller@bu.edu

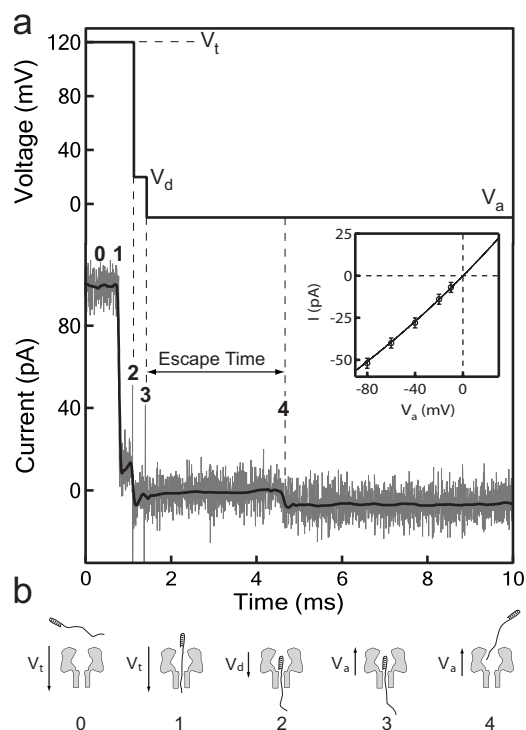


FIG. 1. (a) Dynamic voltage curve (top) and a representative current trace (middle) which probes the escape of a single DNA molecule from the α -HL channel (shown here is HP3', $V_a = -10$ mV). The black filtered line is shown for clarity. (b) Graphical interpretation of different stages of the event shown in (a): A trapping voltage (V_t) is applied (0) until DNA enters the pore stem (1), after which a driving voltage pulse V_d ensures complete hairpin threading (2). An assisting voltage V_a is then applied (3) until the DNA escapes the pore (4). The escape time is defined in the figure. Inset: I - V curve of α -HL at 15 $^{\circ}$ C (trace), and mean currents measured following escape at the indicated assisting voltage values (circles).

hairpins, namely, HP5' and HP3', differ only by the orientation of their poly-(dA)₅₀ tails. The sequences of the two hairpins were as follows: HP3', 3'-GCTCTGTTGCTCTCTCGCAACAGAGC(A)₅₀; HP5', 5'-(A)₅₀CGAGACAACGCTCTCTCGTTGTCTC-G [12]. Before each experiment, the hairpin samples were heated to 75 $^{\circ}$ C for 10 min and then quenched to 4 $^{\circ}$ C. Since the α -HL channel cannot admit duplex DNA into its β -barrel [6,15–17], the overhang tail threads fully until the duplex region reaches the entrance of the barrel. We reconstitute a single α -HL channel in a horizontally supported planar bilayer, as reported elsewhere [10]. All experiments are performed in 1M KCl–10 mM Tris (tris(hydroxymethyl)aminomethane) buffered to a pH of 8.5, at 15.0 \pm 0.1 $^{\circ}$ C. DNA hairpins are introduced to the *cis* chamber (i.e., the vestibule side), and, by convention, a voltage is applied to the *trans* chamber (e.g., a positive voltage will drive DNA from *cis* to *trans*).

Hairpin escape times are probed using a computer-generated dynamic voltage curve, as depicted in Fig. 1(a) [11]. A trapping voltage V_t is applied (point 0) for 300 μ s after the entry of a molecule is detected (1), probed by an

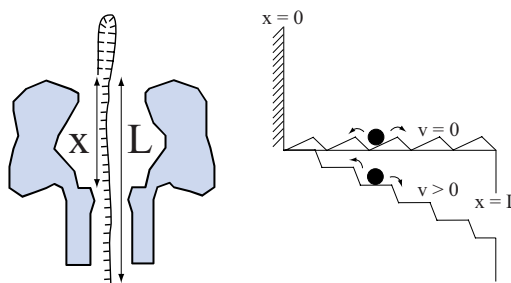


FIG. 2. (Color online) Schematic figure showing a Brownian particle moving in a ratchet potential that models DNA escape from the pore, with and without an applied assisting voltage. The velocities are $v=0$ and $v>0$ for unassisted and assisted motions, respectively. The translocation coordinate is denoted by x and the total hairpin overhang length by L .

abrupt current blockage to the fully blocked state ($\approx 10\%$ of the open pore current). A 300- μ s-long driving pulse V_d (2) is then applied to ensure complete threading [12], followed by a long assisting voltage V_a pulse (3), during which the molecule's escape is probed. Escape is indicated by a sudden change in the current from the fully blocked state to the corresponding open-pore current at $V=V_a$ (see point 4 and inset). At each value of V_a , at least 1500 events were collected for both hairpins, and each event analyzed for the escape time. This directly provides the escape time for each and every threading event. We obtain probability curves for DNA staying in the pore [$P_s(t)$] by integrating the escape time distribution.

The theoretical formulation for calculating $P_s(t)$ is based on work of Lubensky and Nelson [18]. The experimental situation and our Brownian particle representation are schematically shown in Fig. 2. The translocation coordinate, denoted by x , is the separation between the hybridized end of the hairpin and the opening of the α -HL β barrel. Thus, $x=0$ and $x=L$ correspond, respectively, to a fully threaded and an escaped hairpin. In terms of our model, x denotes the position of a Brownian particle. The evolution equation of the probability distribution $P(x,t)$ for the Brownian particle is given by

$$\frac{\partial P}{\partial t} = D \frac{\partial^2 P}{\partial x^2} - v \frac{\partial P}{\partial x}, \quad (1)$$

where D and v are a coarse-grained diffusion constant and the drift velocity, respectively. These transport coefficients, which depend nonlinearly on the applied voltage, reflect the effective microscopic physics at a smaller length scale. Alternatively, $P(x,t)$ represents the probability that a polymer (i.e., the single-stranded DNA) of contour length x , has diffused through the pore at time t . The α -HL channel, which allows only ssDNA to pass through, acts as a reflecting boundary at $x=0$, i.e., the duplex hairpin end. The probability current density $J(x,t)$ thus vanishes at $x=0$,

$$J(x=0,t) = -D \left. \frac{\partial P}{\partial x} \right|_{x=0} + vP(x=0,t) = 0. \quad (2)$$

The probability function $P(x,t)$ must vanish at $x=L$, indicating the end of the translocation process, and is modeled by an absorbing boundary condition

$$P(x=L, t) = 0. \quad (3)$$

We solve Eq. (1) subject to the boundary conditions Eqs. (2) and (3) and initial condition $P(x, t=0) = \delta(x)$, corresponding to a fully threaded hairpin, to obtain $P(x, t)$. Using $P(x, t)$, we then calculate the probability current at the absorbing boundary,

$$\phi(t) = J(x=L, t) = -D\partial_x P(x, t)|_{x=L} + vP(x, t)|_{x=L}. \quad (4)$$

This current gives us the mean first passage time distribution, defined as the distribution of times taken by the Brownian particle to reach the absorbing wall for the first time during its motion [19]. The probability of the particle to stay in the domain $[0, L]$ or, equivalently, the polymer to stay in the pore is related to the mean first passage time distribution by

$$P_s(t) = 1 - \frac{\int_0^t \phi(t) dt}{\int_0^\infty \phi(t) dt}. \quad (5)$$

Our method proceeds by finding the eigenfunction of the operator

$$\mathcal{L}(x, t) = D\frac{\partial^2}{\partial x^2} - v\frac{\partial}{\partial x}. \quad (6)$$

The eigenfunction satisfying the boundary conditions Eqs. (2) and (3) is given by

$$\psi(x, t) = A_k \exp\left(\frac{xv}{2D}\right) \cos(kx) + B_k \exp\left(\frac{xv}{2D}\right) \sin(kx) \quad (7)$$

with an eigenvalue $\lambda = -(v^2 + 4k^2D^2)/4D$. The reflecting boundary condition at the origin and the absorbing boundary condition at $x=L$ demand that

$$\tan(kL) + \frac{2kD}{v} = 0. \quad (8)$$

The boundary conditions, coupled with the normalization condition of the eigenfunction, determine the constants A_k and B_k . We have checked that the coefficients A_k and B_k reduce to the familiar expressions obtained for the diffusion problem in the limit of zero velocity [12], i.e., $A_k = \sqrt{2/L}$ and $B_k = 0$. Using the eigenfunction $\psi(x, t)$, we compute the probability distribution $P(x, t)$ [18]. The expressions for $P(x, t)$, $\phi(t)$, and $P_s(t)$ involve a summation over k values obtained by solving the transcendental equation (8) using the FINDROOT function of MATHEMATICA. The number of k values to be summed over is determined by demanding that the resulting solution $P(x, t)$ satisfies the δ function initial condition. We have used the theory to calculate $P_s(t)$ for positive velocities (assisting voltage).

We also calculate the mean escape time of the hairpin from the pore by generalizing a ‘‘mean time to capture’’ calculation for a diffusing particle by Berg and Purcell [14]. Experimentally, this is a quantity given by the first moment of the escape time distribution. When drift is present, the time to escape, $W(x)$, satisfies

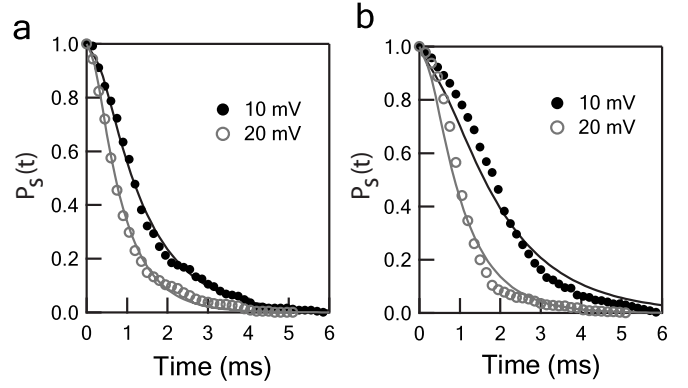


FIG. 3. Experimental (circles) and theoretical (lines) probability distributions of DNA staying in the pore $P_s(t)$ at the indicated assisting voltages ($-V_a$) for (a) HP5' and (b) HP3' hairpins.

$$\frac{d^2W}{dx^2} + \frac{v}{D} \frac{dW}{dx} + \frac{1}{D} = 0, \quad (9)$$

with boundary conditions $(dW/dx)|_{x=0} = 0$ and $W(x=L) = 0$. Solving Eq. (9) with the boundary conditions leads to

$$W(x) = \frac{L-x}{v} - \frac{D}{v^2} [\exp(-vx/D) - \exp(-vL/D)], \quad (10)$$

with $x=0$ corresponding to our situation, where the hairpin is fully threaded at $t=0$. Note that the first term is just the ballistic capture time. When $D \ll Lv$, this term dominates over most of the interval $0 < x < L$, except within a small distance $\delta = D/v$ of the boundaries.

Figure 3 shows the experimental $P_s(t)$ for HP5' and HP3' with applied voltages $-V_a = 10$ and 20 mV, represented by solid and open circles, respectively. The solid lines are best theoretical fits to the data, from which D and v are recovered. First, it is observed that the $P_s(t)$ curves vanish at longer times for HP3' than for HP5' at both voltages, as previously observed under no bias [12]. Second, $P_s(t)$ for HP5' is in excellent agreement with theory, while for HP3' the data cannot fit the theoretical curves better than within 5% and 10% for HP5' and HP3', respectively.

We attribute the observed deviations between our theory and experiments for HP3' threading to orientation-dependent interactions with the α -HL pore: (1) HP3' escape at the low-bias regime is up to 60% slower than HP5' escape, (2) the current blockage amplitude for 3'-threaded DNA is larger than for 5'-threaded DNA, indicating a ‘‘tighter’’ fit. Our two-parameter model, which does not explicitly take into account DNA-pore interactions, is therefore sufficient to extract meaningful values for D and v .

Our main findings, summarized in Table I, show the experimentally measured and theoretically calculated mean escape times with D and v values that best fit the experimental $P_s(t)$ curves. We find that, for a given applied voltage, the velocities for HP3' and HP5' are approximately the same, perhaps reflecting a similar effective charge for both hairpins. On the contrary, the D values differ widely for each orientation. Furthermore, the diffusion constants for both hairpins monotonically increase with the applied assisting

TABLE I. Comparison of experimental and theoretical mean escape times, and the extracted diffusion coefficients and velocities for HP3' and HP5'.

DNA type	$-V_a$ (mV)	$\langle t \rangle_{\text{expt}}$ (ms)	$\langle t \rangle_{\text{calc}}$ (ms)	$D \times 10^{-10}$ (cm ² /s)	$v \times 10^{-4}$ (cm/s)
HP3'	0	15.0	14.7	1.8	
	10	2.5	2.5	4.9	6.5
	20	1.3	1.2	13.5	9.5
HP5'	0	8.8	8.8	3.1	
	10	1.6	1.6	11.0	6.8
	20	1.2	1.1	19.0	9.5

voltage. Since diffusion is associated with hopping over energy barriers created by interactions of DNA with the α -HL channel, it is most sensitive to the orientation of ssDNA at small biases. The monotonic increase of D with the applied bias suggests a voltage-induced reduction of the translocation energy barrier, facilitating activated jumps. When the applied bias is very high ($-V_a > 20$ mV), the overall tilt of the potential is such that the microscopic ratchetlike potential ceases to matter, and we expect a loss of orientation sensitivity and drift-dominated motion of the DNA.

Figure 4 shows the variation of mean escape times as a function of the applied bias. For zero applied bias, the mean escape time ratios of HP3' to HP5' is ≈ 1.7 [12]. The ratio gradually decreases with increasing voltage. At larger assisting voltages, i.e., $-V_a > 20$ mV, we observe mean escape time ratios of nearly 1, indicating a loss of orientation sensitivity. Physically, these results imply a bias-induced conformational change in the DNA- α -HL interaction, or, formulated differently, a superlinear perturbation in the underlying energy landscape of DNA-channel interaction in this voltage regime is observed, explaining the deviation from the simple diffusion and drift model.

In conclusion, we have explored the voltage-dependent interactions of ssDNA with the α -HL channel by directly probing the escape dynamics of individual DNA molecules. Using a coarse-grained model, we developed a two-parameter, closed-form expression for the probability distribution of the DNA staying in the pore. Fitting our experimental observations to our theory, we back out bias-dependent drift velocities and diffusion constants. We also calculate theoretically the mean escape time of a polymer from a pore and fit it to the first moment of the distribution of translocation times. At high assisting voltages, we find that the orientation dependence disappears, which we attribute to

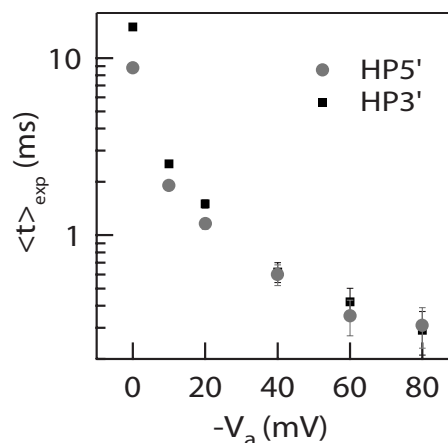


FIG. 4. Semilogarithmic plot of the experimental mean escape times for 3' (gray circles) and 5' (black squares) hairpins with applied bias, showing loss of orientation selectivity at ($-V_a > 20$ mV).

tilting of the microscopic DNA-channel interaction potential. We also find that 5' retraction is facilitated over 3' at any applied assisting voltage, and conjecture that the packing and orientation of DNA bases in the channel induce different DNA-channel interactions for the two orientations.

Despite agreement at low assisting voltages for 5'-oriented threading, our two-parameter hydrodynamic theory yields poor fits to experimental $P_s(t)$ curves for 3' threading. We believe that 3'-oriented DNA forms extensive secondary contacts with the channel, resulting in additional distortion of the probability curve. A more sophisticated theory, which incorporates a shallow potential well near the reflecting wall, may be used to model this and in turn yield better fits to experimental data. The failure at high assisting voltages might be attributed to drift-induced interactions as well as conformational changes of the pore itself, which our theory does not account for. However, any modification of the simple coarse-grained theory introduces new phenomenological parameters, that are either not calculable within the model, or have not been determined experimentally. We hope that this work will inspire further numerical and experimental work in this direction.

The authors acknowledge the NSF Grant No. NIRT 0403891 and NIH Grant No. GM075893 for financial support. B.C. and D.R.N. acknowledge support from the Harvard MRSEC through Grant No. DMR0213805. B.C. thanks Harvard NNIN for computational resources.

[1] J. J. Kasianowicz, E. Brandin, D. Branton, and D. W. Deamer, Proc. Natl. Acad. Sci. U.S.A. **93**, 13770 (1996).
 [2] A. Meller, L. Nivon, E. Brandin, J. Golovchenko, and D. Branton, Proc. Natl. Acad. Sci. U.S.A. **97**, 1079 (2000).
 [3] M. Akesson, D. Branton, J. Kasianowicz, E. Brandin, and D. Deamer, Biophys. J. **77**, 3227 (1999).

[4] A. Meller, J. Phys.: Condens. Matter **15**, R581 (2003).
 [5] E. Slonkina and A. B. Kolomeisky, J. Chem. Phys. **118**, 7112 (2003).
 [6] L. Song, M. Hobaugh, C. Shustak, S. Cheley, H. Bayley, and J. Gouaux, Science **274**, 1859 (1996).
 [7] H. Bayley, Curr. Opin. Chem. Biol. **10**, 628 (2006).

- [8] M. Rhee and M. A. Burns, Trends Biotechnol. **24**, 580 (2006).
- [9] G. V. Soni and A. Meller, Clin. Chem. **53**, 1996 (2007).
- [10] A. Meller, L. Nivon, and D. Branton, Phys. Rev. Lett. **86**, 3435 (2001).
- [11] M. Bates, M. Burns, and A. Meller, Biophys. J. **84**, 2366 (2003).
- [12] J. Mathé, A. Aksimentiev, D. R. Nelson, K. Schulten, and A. Meller, Proc. Natl. Acad. Sci. U.S.A. **102**, 12377 (2005).
- [13] R. C. Lua and A. Y. Grosberg, Phys. Rev. E **72**, 061918 (2005).
- [14] H. Berg, *Random Walks in Biology* (Princeton University Press, Princeton, NJ, 1993); H. Berg and E. M. Purcell, Biophys. J. **20**, 193 (1977).
- [15] W. A. Vercoutere, S. Winters-Hilt, H. Olsen, D. Deamer, D. Hausseler, and M. Akeson, Nat. Biotechnol. **19**, 248 (2001).
- [16] A. F. Sauer-Budge, J. A. Nyamwanda, D. K. Lubensky, and D. Branton, Phys. Rev. Lett. **90**, 238101 (2003).
- [17] J. Mathé, H. Visram, V. Viasnoff, Y. Rabin, and A. Meller, Biophys. J. **87**, 3205 (2004).
- [18] D. K. Lubensky and D. R. Nelson, Biophys. J. **77**, 1824 (1999).
- [19] H. Risken, *The Fokker-Planck Equation* (Springer-Verlag, Berlin, 1984).